Supporting Information

Near-Infrared Heterojunction Field Modulated Phototransistors with Distinct Photodetection/Photostorage Switching Feature for Artificial Visuals

Jiayue Han,[†,a] Xiaoyang Du,[†,a] Zhenhan Zhang,[†,b,c] Zeyu He,[a] Chao Han,[a] Runzhang Xie,[c] Fang Wang,[,c] Silu Tao,*[,a] Weida Hu,[c] Chongxin Shan,[d] Ming Yang,[a] Jun Gou,[a,e] Zhiming Wu,[a,e] Yadong Jiang[a,e] and Jun Wang*[,a,e]*

a, School of Optoelectronic Science and Engineering, University of Electronic Science and Technology of China, Chengdu 610054, China
E-mail: silutao@uestc.edu.cn

b, State Key Laboratory of ASIC and System, School of Microelectronics, Fudan University, Shanghai, China.

c, State Key Laboratory of Infrared Physics, Shanghai Institute of Technical Physics, Chinese Academy of Science, 500 Yutian Road, Shanghai 200083, China

d, Henan Key Laboratory of Diamond Optoelectronic Materials and Devices, School of Physics and Engineering, Zhengzhou University, Zhengzhou 450001, China

e, State Key Laboratory of Electronic Thin Films and Integrated Devices, University of Electronic Science and Technology of China, Chengdu 610054, China

E-mail: silutao@uestc.edu.cn
E-mail: fwang@mail.sitp.ac.cn
E-mail: wjun@uestc.edu.cn

†These authors contributed equally to this work.

1. The optical microscope image of graphene/ZnO on SiO_2 substrate.

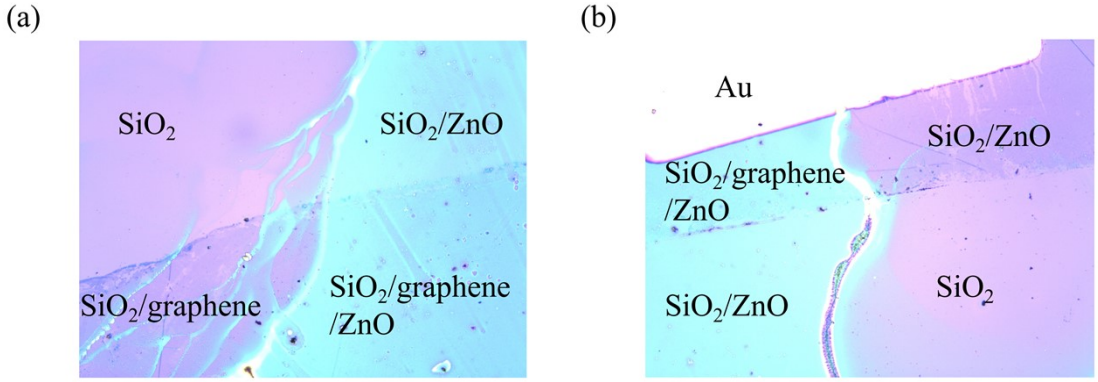

Fig. S1. (a,b) Optical microscope image of graphene/ZnO on SiO_2 substrate.

2. The Raman spectrum characterization.

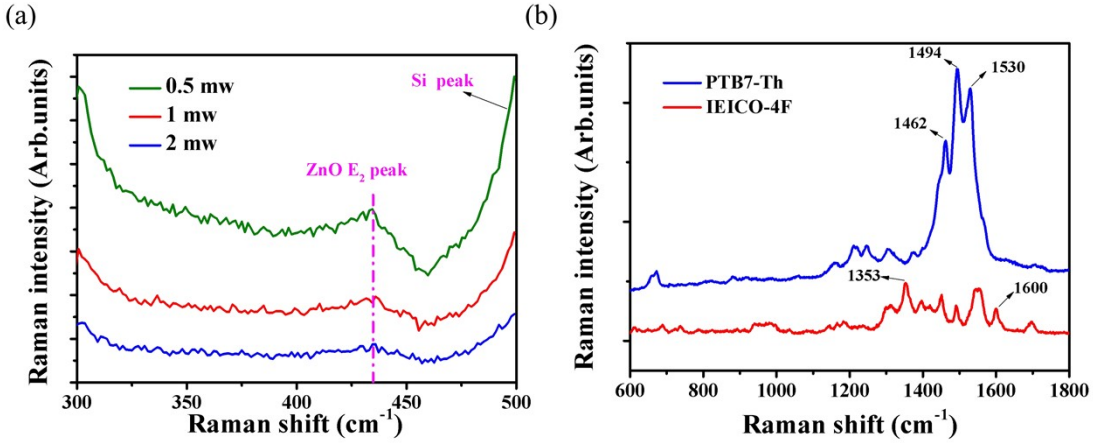

Fig. S2. (a) Raman spectra for different light intensity powers of ZnO on SiO_2 substrate, (b) Raman spectra for PTB7-Th and IEICO-4F films.

3. The wavelengths photocurrents with 10 V V_g applying.

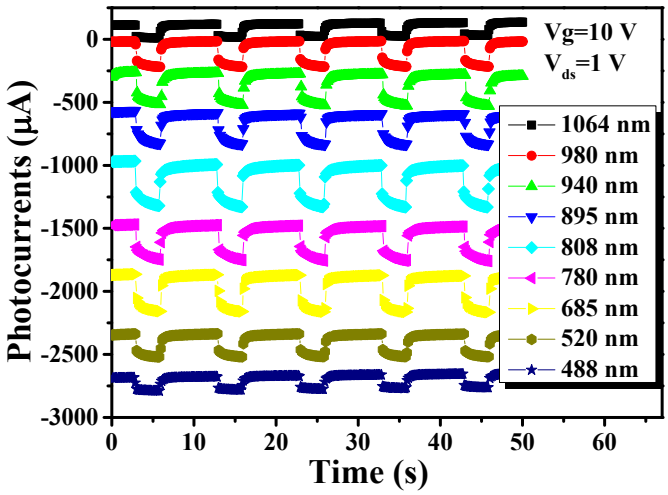

Fig. S3. The time-resolved photocurrents measurement under the wavelengths from 488 to 1064 nm. Power density=10 mW/cm^2.

4. The photocurrents and responsivity comparison with different control structures.

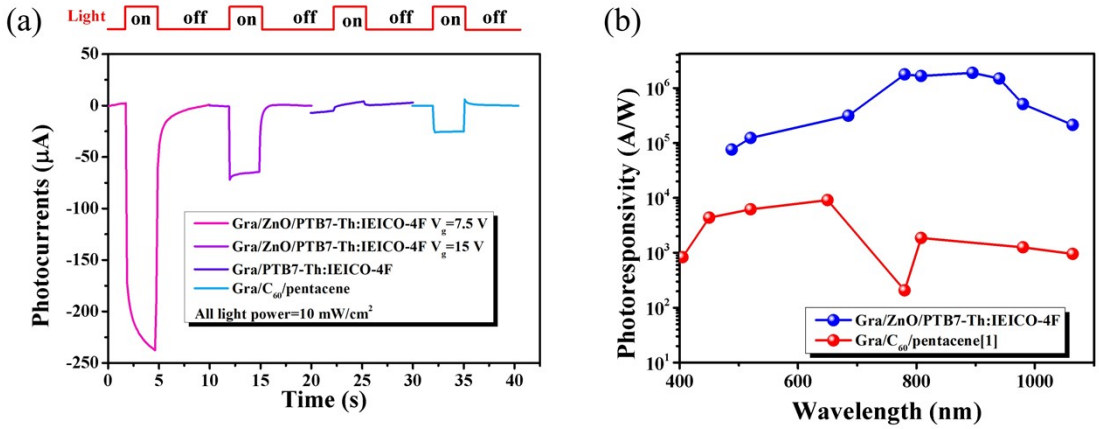

Fig. S4. (a) The photocurrent comparison with different device structures and the same input power density. (b) The photo-responsivity of graphene/ZnO/PTB7-Th:IEICO-4F and graphene/C_{60}/pentacene.[1]

5. The photocurrents and I-V character with different V_g applying.

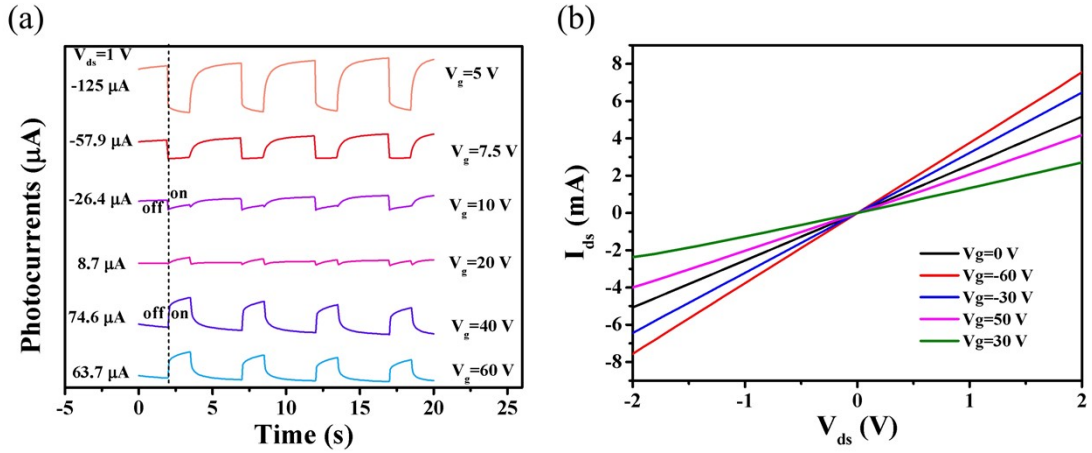

Fig. S5. (a) Transient photocurrent measurements with different gate voltages under the illumination of 940 nm light. Power density of 940 nm is 377 μW/cm^2. (b) The I-V curve with different Vg values under the illumination of 808 nm, power density of 808 nm is about 60 mW/cm^2.

6.Transport Parameters calculation

S6

The carrier mobility μ of graphene/ZnO/PTB7-Th:IEICO-4F heterojunction is estimated by equation :

$$\mu = \frac{L}{WC_{ox}V_{ds}} \times \frac{\partial I_{ds}}{\partial V_g}$$

Where the L and W are respectively the length and width of channel, the C_{ox} represents the geometric capacitance of bottom gate (285 nm SiO_2) using 12.5 nF/cm^2, V_{ds} is the bias under the channel and $\frac{\partial I_{ds}}{\partial V_g}$ stands for gradient relation of I_{ds}-V_g ($\frac{\partial I_{ds}}{\partial V_g}$ obtained from **Fig.** 2c dark curve from -30 V to 20 V). As the result, the μ is computed to be 984 cm^2/V^{-1}S^{-1}

7. Photoresponse performance and 1/f noise with the variation of Vg.

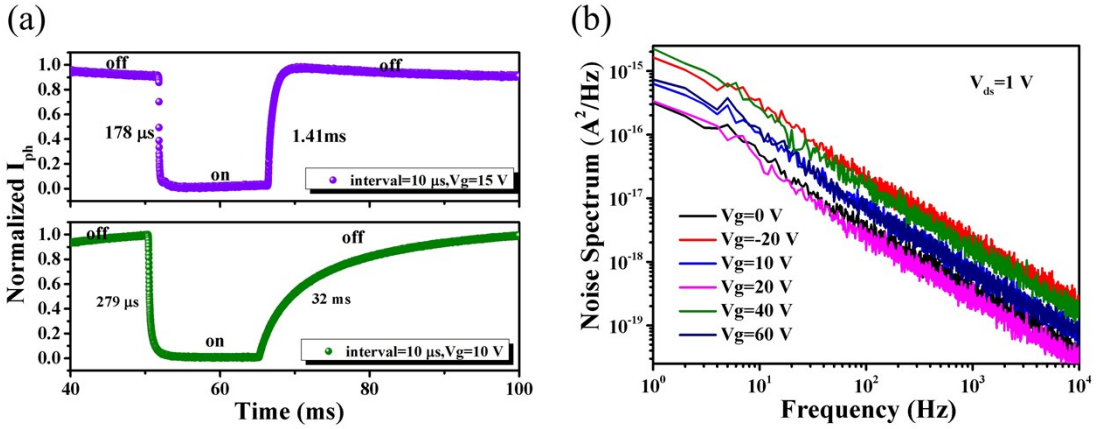

Fig. S7. (a) The highly time-resolved photocurrent measurement with interval 10 μs at the gate voltage of 10 V and 15 V. Power density of 895 nm is 263 μW/cm^2 (b) The 1/f noise analysis of the device for different V_{ds} values.

8. Photoresponse performance with the variation of operated frequency.

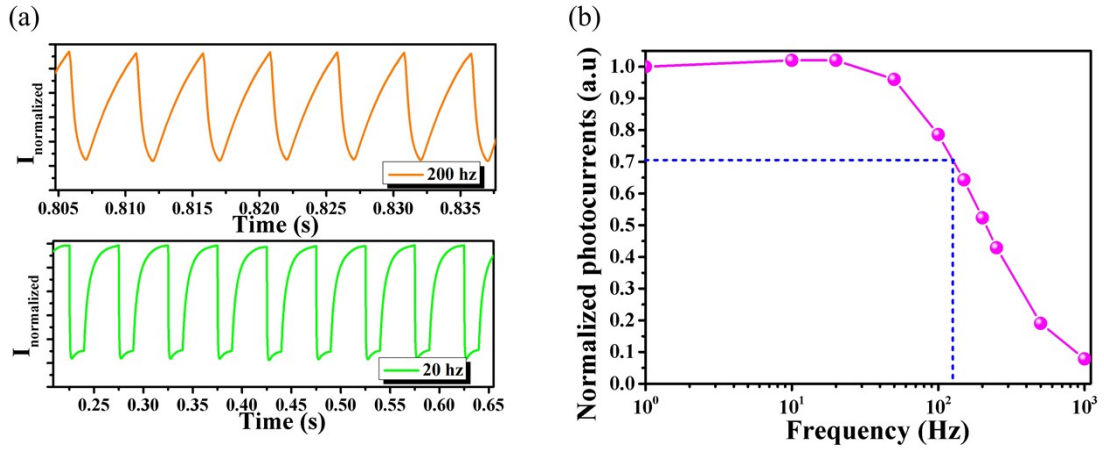

Fig. S8. (a) The time-resolved responses of 895 nm under the light on-off frequency of 20 Hz and 200 Hz. (b) The normalized photocurrents with the variation of light on-off frequency.

9. The photo-storage character of graphene/ZnO/PTB7-Th:IEICO-4F device.

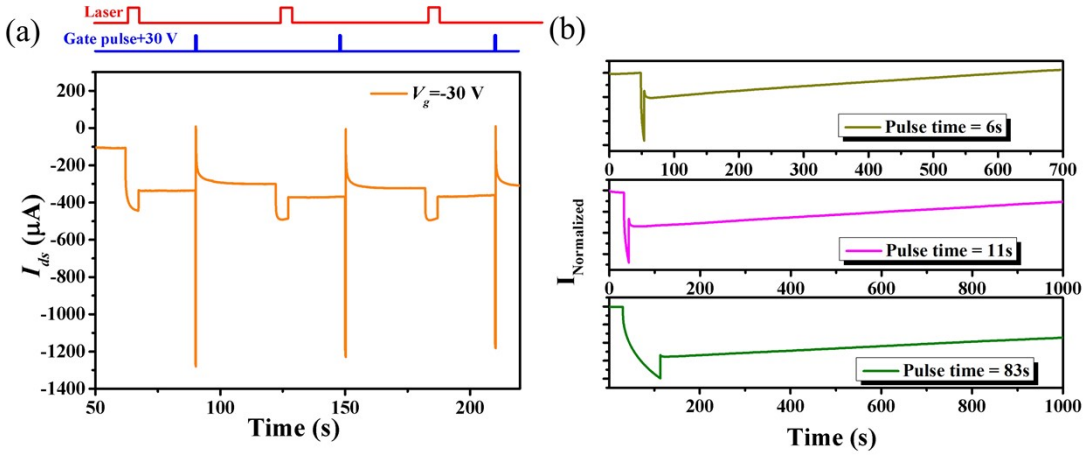

Fig. S9. (a) The photocurrents on-off switching operation with +30 V gate pulse (pulse width= 0.25 s) for erasing. The power density of the 895 nm input laser is 20 mW/cm^2. (b) The 940 nm photo-memory persistent states at three different pulse time widths. Vg=-20 V.

10. The exposure time dependent photo-storage feature.

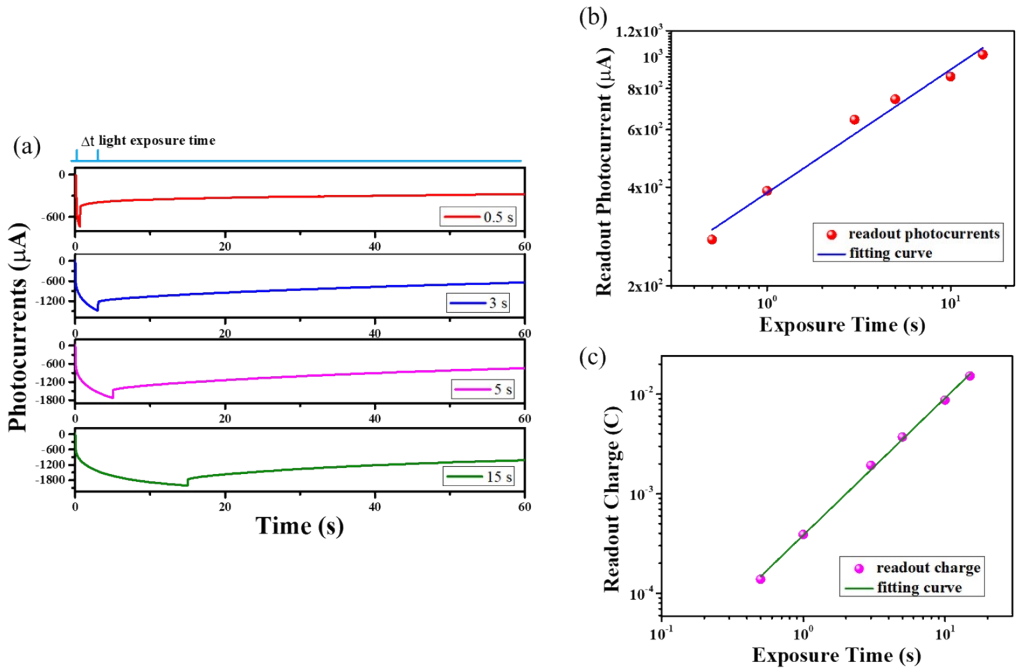

Figure S10 The memory features as a function of exposure time. (a) Time-dependent memory currents with different light exposure times. (b) The readout photocurrents with various light exposure times. (c) The readout charge with various light exposure times.

11. The response and memory features as a function of BHJ thickness.

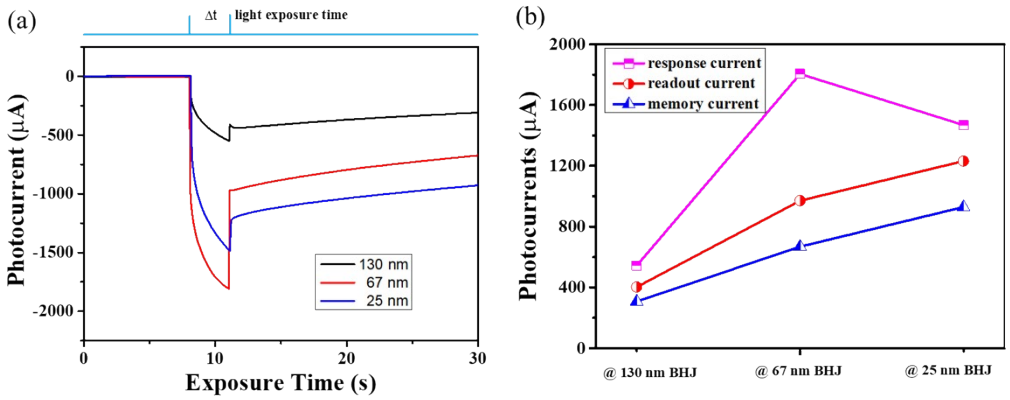

Figure S11 The response and memory features as a function of BHJ thickness. (a) Time resolved response and memory currents. (b) The response and memory features with various BHJ thickness.

Although, the blend heterojunction ensures the dissociation efficiency and promote the QE, which allows thicker photosensitive layer for higher response current. But the excessive thick of the active layer may affect the light absorption of the under layer closed to the graphene and photo-generated carriers in upper layer due to the effective exciton distance. Thus, a relative low response current in 130 nm BHJ. And the middle thickness (67 nm BHJ) device shows a relatively low memory results both in readout current and memory current.

Reference

[1] Han, J. et al. Graphene/Organic Semiconductor Heterojunction Phototransistors with Broadband and Bi-directional Photoresponse. Adv Mater 30, 1804020, doi:10.1002/adma.201804020 (2018).